Malaysian Journal of Analytical Sciences, Vol 23 No 4 (2019): 690 - 702
DOI: https://doi.org/10.17576/mjas-2019-2304-16

MALAYSIAN JOURNAL OF ANALYTICAL SCIENCES
Published by The Malaysian Analytical Sciences Society
ISSN 1394 - 2506

SYNTHESIS AND BINDING PROPERTIES OF TERT-BUTYL AMIDE MACROCYCLES FOR PSEUDOROTAXANES FORMATION

(Sintesis dan Sifat Pengikatan Makrosiklik Tetrabutil-Amida bagi Penghasilan Pseudorotazen)

Nurul Izzaty Hassan[1]* and Douglas Philp[2]

[1]Center for Advanced Material & Renewable Resources,
Faculty of Science and Technology
Universiti Kebangsaan Malaysia, 43600 UKM Bangi, Selangor, Malaysia
[2]Department of Chemistry,
Northwestern University, 2145 Sheridan Road, Evanston, IL 60208-3113, USA

**Corresponding author: drizz@ukm.edu.my*

Received: 31 March 2018; Accepted: 17 April 2019

Abstract

The tert-butyl amide macrocycle containing ethylene glycol moiety (cMDG) was constructed starting from 5-tert-butylisophthalic acid **1** which was activated to acid chloride derivative **2** using thionyl chloride in toluene. Further, the synthesis of the second macrocycle based on pyridine framework (cMP) was achieved in similar way before coupled to the diamine derivative **4**. Following that, the compound's electronic structure was calculated using simple molecular mechanics calculation to represent the preferable conformation of these macrocycles. In order to evaluate the influence of the benzene ring in the framework of both macrocycles to complex the guests, the following binding experiments were carried out with the synthesized maleimide **5** and CF_3 maleimide **6**. An equimolar mixture of macrocycle cMDG and maleimide **5** or **6** in $CdCl_3$ was prepared and analysed by ^1H and ^{19}F NMR spectroscopy, respectively. The similar binding experiments were then carried out with macrocycle cMP. The association constant, K_a for the complexation of pseudorotaxane [cMDG·5] and [cMP·5] were estimated to be 190 ± 20 M^{-1} and 160 ± 20 M^{-1}, respectively. On contrary, the association constant for the complexation of pseudorotaxane [cMDG·6] and [cMP·6] complexes were enhanced with a K_a value of 1000 ± 100 M^{-1} and 460 ± 50 M^{-1} at 25 °C in $CdCl_3$. In addition, the ^1H and ^{19}F NMR spectra of these macrocycles and maleimides showed complexes are in slow exchange on the ^1H NMR chemical shift timescale. This can be attributed to significant binding events of pseudorotaxane complexes, compare to the free species observed in isolation. In the case of slow exchange, the K_a was determined using the single-point method.

Keywords: macrocylic, ethylene glycol, pyridine, pseudorotaxane

Abstrak

Makrosiklik tetra-butil amida yang mengandungi moieti etilena glikol (cMDG) disintesis bermula dari pengaktifan asid 5-tetrabutilisoftalik **1** kepada sebatian asid klorida **2** menggunakan tionil klorida dalam pelarut toluena. Sebatian perantara ini kemudiannya ditambah kepada sebatian bis amina **3** untuk menghasilkan makrosiklik cMDG melalui sintesis pencairan tinggi. Selain itu, sintesis makrosiklik kedua berasaskan kerangka pyridina (cMP) turut dicapai melalui cara yang sama sebelum ditambah kepada sebatian terbitan diamina **4**. Berikutan itu, struktur elektronik makrosiklik dikira menggunakan pengiraan molekular mekanik asas bagi mendapatkan gambaran konformasi yang sesuai. Untuk menilai pengaruh gelang benzena dalam moeiti makrosiklik untuk pengkompleksan dengan tetamu, kajian pengikatan telah dijalankan menggunakan sebatian maleimida **5** dan CF_3 maleimida **6** yang telah disintesis terlebih dahulu. Satu campuran dengan kemolaran yang sama di antara makrosiklik cMDG dan maleimida **5** atau **6** dalam pelarut $CdCl_3$ disediakan dan dianalisa menggunakan ^1H dan ^{19}F RMN spektroskopi. Kajian pengikatan yang sama turut dijalankan menggunakan makrosiklik cMP. Nilai pemalar pengikatan, K_a bagi kompleks pseudorotazen [cMDG·5] dan [cMP·5] telah dianggarkan sebanyak 190 ± 20 M^{-1} dan 160 ± 20 M^{-1}, masing-masing. Sebaliknya, kekuatan pengikatan semakin meningkat bagi perkompleksan pseudorotazen [cMDG·6] dan [cMP·6] di mana nilai K_a yang

diperolehi ialah 1000 ± 100 M^{-1} dan 460 ± 50 M^{-1} pada 25 ° C dalam pelarut $CdCl_3$. Di samping itu, ^1H dan ^{19}F RMN spektra bagi sebatian makrosiklik dan maleimida menunjukkan kompleks dalam pertukaran lambat pada 1H NMR anjakan kimia. Ini boleh dikaitkan dengan proses pengikatan signifikan pada kompleks pseudorotazen berbanding sebatian yang tidak berikatan. Nilai K_a ditentukan menggunakan kaedah titik tunggal bagi kes pertukaran lambat.

Kata kunci: makrosikilik, etilena glikol, piridina, pseudorotazen

Introduction

A common retrosynthetic disconnection shared by generic [2]-rotaxane and [2]-catenane structures revolves around in the [2]-pseudorotaxane precursor, in which a linear molecule is threaded through a macrocyclic unit. Thus, they are similar to rotaxane structure with the exception that the linear molecule not terminated by the two bulky stoppers. Further modification of this precursor can possibly proceed in two ways, by virtue of (a) stoppering the end linear component with sufficient large groups, results in the formation of [2]-rotaxane or (b) macrocyclisation of the linear component to affords to [2]-catenane (Figure 1).

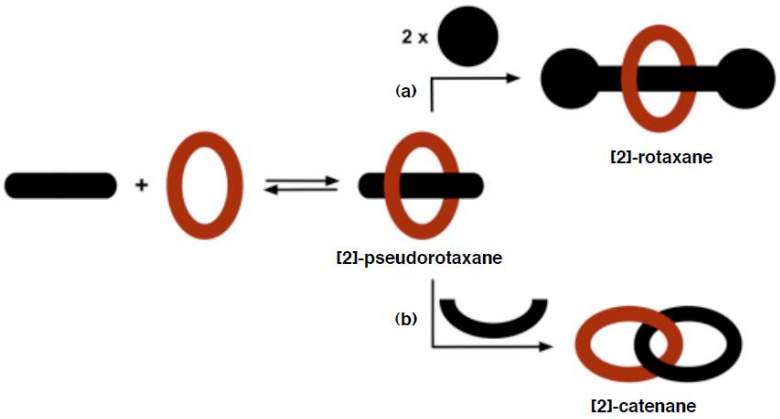

Figure 1. Graphical representation of the synthesis of (a) [2]-rotaxane by means of stoppering the linear component with two bulky end groups and (b) [2]-catenane by means of macrocyclisation of the linear component of the similar precursor

Prospective guests such as pyridone, urea and amide have been identified to probe as the binding components. Upon addition of a guest in the linear component and macrocycle with the complementary binding motifs, the equilibrium is established. The macrocycle is constantly being displaced from the binding site in the linear component, which resulted in two species, namely the [2]-pseudorotaxane complex and guest distinguishable in situ (Figure 2). The stability of the [2]-pseudorotaxane complex is defined by the association constants, K_a. The association constant relates to the affinity of the macrocycle to associate the binding site of the guest and can be varied by manipulating the temperature, based on the free energy Gibbs. In the case of low temperature, a substantial amount of the [2]-pseudorotaxane are obtained as a results of increase value of K_a [1]. A large association constant corresponds to a high equilibrium concentration of bound guest and hence more stable or tighter the preorganization of the [2]-pseudorotaxane complex. Undoubtedly, a high association constant of [2]-pseudorotaxane complex is mandatory to ensure a significant amount of rotaxane is synthesized.

An anion-directed pseudorotaxanes has been reported by Beer and co-workers [2]. The zwitterion comprised Crabtree-type pyridinium clef binding a chloride [3,4] with amide macrocycle results in the formation of a pseudorotaxane in acetone-d_6 with an association constant, K_a of 2400 M^{-1}. The pseudorotaxane is stabilized by chloride-NH hydrogen bonds, π-π stacking interaction and C-H···hydrogen bonds. A vast consideration has been given to the potential use of pseudorotaxanes in molecular devices [5] such as switches by means of external stimulus such as chemical [6], electrochemical [7] or photochemical [8].

One of the most important tasks in the formation of macrocycle is the key macrocyclisation step. In the absence of a suitable template, the synthesis of macrocyclic component employs the high-dilution conditions [9]. The high dilution approaches [10] have been used in a large number of macrocyclic syntheses. One rationale behind this strategy is that in dilute solution, the formation of the cyclic product by intramolecular reaction is more likely and thus faster than formation of a polymer, which requires a collision between two different starting reagents by means of intermolecular reaction. Furthermore, if the cyclisation is intrinsically faster than the rate of addition of the starting reagents, then the concentration of the reactants will always be small and not increase during the course of the reaction [11]. These approaches have been taken to assemble the macrocycle skeleton in this paper. A prototype amide-based macrocycle has been extensively [12-14] explored as the macrocyclic unit within our group and others. Nevertheless, the binding affinity shown in previous work [15] is moderate as a consequence of diminutive cavity and hence, decreasing the association constant, K_a in the [2]-pseudorotaxane complex. Herein, two tert-butyl amide-based macrocycles are proposed using high-dilution technique and analysed its binding properties with two respective guests. The existing complementary motif between hydrogen bond donor and acceptor are maintained in the new macrocycle framework.

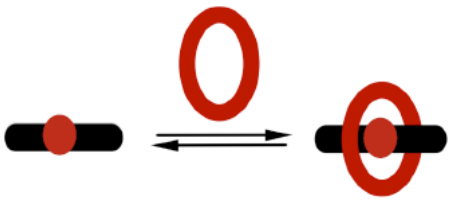

Figure 2. The reversible formation of the [2]-pseudorotaxane complex

Materials and Methods

Chemicals

5-tert-butylisophthalic acid, 4-(bromomethyl)benzonitrile, sodium hydride, diethylene glycol, thionyl chloride, trimethylamine, hydrochloric acid, potassium hydroxide, magnesium sulphate, BH_3·THF complex (1M solution in THF), 2,6-pyridine dimethanol,3,5-dimethylbenzoic acid, 4,4'-ethylene dianiline, sodium hydrogen carbonate, brine, maleic anhydride, zinc bromide, hexamethyldisilazone, 3,5-bis(trifluoromethyl)benzoyl chloride were purchased from ABCR GmbH & Co, Alfa-Aesar, Apollo Scientific Ltd., Avocado research Chemicals Ltd Fisher Scientific UK Ltd., Sigma-Aldrich company Ltd. or VWR International Ltd. and were used as received or otherwise purified by standard techniques where required. Most of non-aqueous reactions were carried out under an inert argon or nitrogen atmosphere with the inert gas passing through a bed of 4 Å molecular sieves and self-indicating silica gel. Brine refers to a saturated aqueous solution of sodium chloride. Anhydrous solvents were obtained under the following conditions, such as dry MeCN was distilled from calcium hydride in a recycling still, dry CH_2Cl_2 was obtained using a MBRAUN GmbH MB SPS-800 solvent purification system, which the solvent was dried by passage through filter columns and dispensed under an atmosphere of Ar or N_2 gas, $CdCl_3$ was neutralised over $CaCl_2$ filtered and stored over 4 Å activated molecular sieves and dry THF was distilled from sodium in a recycling still using benzophenone kethyl as indicator.

Chemical characterization

Analytical thin layer chromatography (TLC) analysis was performed on MACHEREY-NAGEL GmbH & Co, POLYGRAM® SIL G/UV254 plates, plastic backed 0.2 mm silica gel plates with fluorescent indicator. Developed plates were air-dried and visualized under UV lamp (λ_{max} 254 or 366 nm) or incubating with iodine on sand. Where necessary, thermal development after dipping in methanolic DNP and sulfuric acid solution and ninhydrin in *n*-butanol or a solution of aqueous potassium permanganate, was used to aid visualization. Flash Column chromatography and silica plugs were carried out on Apollo Scientific Ltd. Silica gel 40-63 micron or Silicycle

SiliaFash® P60 silica gel (230-400 mesh) eluting with solvents as supplied under a positive pressure of compressed air. Melting points were measured in open capillary tubes using an Electrothermal 9200 melting point apparatus and are uncorrected. Mass spectra were recorded on a Micromass GCT spectrometer for electron impact (EI) operating at 70 eV or chemical ionization (CI) using isobutane as the ionising gas. Electrospray ionisation spectra (ES) were performed on a Micromass LCT spectrometer operating in positive or negative mode from solutions of methanol, acetonitrile or water. *m/z* values are reported in Daltons and followed by their percentage abundance in parentheses.

General NMR spectroscopy procedures

^{1}H NMR spectra were recorded on a Bruker Avance 300 (300.1 MHz), a Bruker Avance II 400 (400.1 MHz), a Bruker Avance 500 (499.9 MHz) or a Varian UNITYplus 500 (500.1 MHz) spectrometer using the deuterated solvent as the lock and the residual spectra as the internal reference in all cases. The chemical shift information (δ_H) for each resonance signal is given in units of parts per million (ppm) relative to trimethylsilane (TMS) where δ_H TMS = 0.00. The number of protons (n) for a reported resonances signal are indicated from their integral value and their multiplicity are represented by the symbols s, d, t, q, m and br which denote singlet, doublet, triplet, quartet, multiplet and broad singlet, respectively. Their coupling constant (*J*) are determined by analysis using iNMR© (Version 3.6.3, Mestrelab Research, 2010) and quoted to the nearest 0.1 Hz. Identical coupling constants are averaged in each spectrum and also reported to the nearest 0.1 Hz. ^{13}C NMR spectra were recorded on a Bruker Avance 300 (75.5 MHz), a Bruker Avance II 400 (100.6 MHz) or a Bruker Avance 500 (125.7 MHz) spectrometer utilizing the DEPTQ pulse sequences with broadband proton decoupling using the deuterated solvents as the lock and the residual solvent as the internal reference in all cases. In the assignment of ^{13}C NMR spectra, the chemical shift information (δ_C) for each resonance signal are given in units of parts per million (ppm) relative to trimethylsilane (TMS) where δ_C TMS = 0.00. Mainly, the signals are singlets or unless stated, which their multiplicity is represented by the symbol d for doublet. ^{19}F NMR spectra were recorded using a Bruker Avance 300 (282.4 MHz), a Bruker Avance II 400 (376.5 MHz) or a Bruker Avance 500 (470.3 MHz) spectrometer using a broadband proton decoupling pulse sequence with the deuterated solvent as the internal lock. The chemical shift information (δ_F) for each resonance signal are given in units of parts per million (ppm) relative to CCl_3F where δ_F CCl_3F = 0.00. The analysis of ^{1}H, ^{13}C and ^{19}F spectra were carried out using iNMR© software (Version 3.6.3, Mestrelab Research, 2010).

Determination of binding constants

In the case of fast exchange (F) on the NMR chemical shift timescale between the complexed and uncomplexed species, the change in the observed chemical shift for discrete resonance is a weighted average between the bound and unbound species. The association constant, K_a was determined by NMR titration method using ^{1}H NMR spectroscopy at 298 K. The stock solutions and samples were made up in dry $CdCl_3$ using volumetric flask (accuracy ± 0.02 mL). In a typical ^{1}H NMR titration experiment, small aliquots of guest are added to a solution of host of known concentration and the NMR spectrum of the sample monitored as a function of guest concentration. Various atomic nuclei are often reported for their changes in chemical shift. The binding constant is extracted from the titration curve, which is the plot of changes in chemical shift against added guest concentration by fitting the curve using a non-linear curvefitting program. However, if the exchange of bound and unbound species is slow (S) on the NMR chemical shift timescale, then the association constant is estimated by simple integration of the ^{1}H and ^{19}F NMR resonances for bound and unbound host or guest, so called the single-point method.

Computational methods

All molecular mechanics calculations were performed on a Linux workstation using the OPLS2005 forcefield together with the GB/SA solvation model for chloroform as implemented in Macromodel (Version 9.8, Schrödinger Inc., 2010). Electronic structure calculations were carried out using MOPAC2009 running on a Linux cluster [16, 17].

5-*tert*-Butylisophthaloyl dichloride 2

5-*tert*-butylisophtalic acid **1** (2.0 g, 9.0 mmol) was suspended in toluene (45 mL) together with thionyl chloride (0.72 mL, 18.0 mmol) and refluxed at 80 °C for 18 h. An excess of thionyl chloride was distilled off by the azeotropic distillation with toluene to furnish dark yellow oil (2.28 g, 98%) as desired product. This product was used in the next step without further purification. ^{1}H NMR (300.1 MHz, $CdCl_3$) : δ_H 8.69 (1H, t, $^{4}J_{HH}$ 1.6 Hz; Ar*H*),

8.40 (2H, d, $^4J_{HH}$ 1.7 Hz; 2 × Ar*H*), 1.41 (9H, s; 3 × C*H*$_3$); ^{13}C NMR (75.5 MHz, $CdCl_3$) : δ_C 167.8 (*C*OCl), 154.1 (Ar*C*), 134.4 (Ar*C*), 134.2 (Ar*C*H), 131.8 (Ar*C*H), 35.5 (q*C*), 31.1 (*C*H$_3$); MS (ES^+) *m/z* 273.1 ([M+H]$^+$, 100), 477 (20).

(4,4'-(2,2'-Oxybis(ethane-2,1-diyl)bis(oxy))bis(methylene)bis(4,1-phenylene))dimethanamine 3
^{1}H NMR (300.1 MHz, $CdCl_3$): δ_H 7.31 (4H, d, $^3J_{HH}$ 8.2 Hz; 4 ×ArH), 7.26 (4H, d, $^3J_{HH}$ 8.2 Hz; 4 × ArH), 4.55 (4H, s; 2 × CH_2), 3.85 (4H, s; 2 × CH_2), 3.70 – 3.61 (8H, m; 4 × CH_2), 1.60 (4H, br s; 2 × NH_2); ^{13}C NMR (75.5 MHz, $CdCl_3$): δ_C 142.8 (ArC), 136.9 (ArCH), 128.2 (ArCH), 127.2 (ArC), 73.1 (CH_2), 70.8 (CH_2), 69.5 (CH_2), 46.4 (CH_2); MS (CI^+) m/z 105 (22), 119 (46), 120 (100), 328 (20), 345 ([M+H]$^+$, 12); HRMS (CI^+) m/z calculated for $C_{20}H_{29}N_2O_3$ [M+H]$^+$ 345.2178, found 345.2177.

(4,4'-Pyridine-2,6-diylbis(methylene))bis(oxy)bis(methylene)bis(4,1-phenylene))dimethanamine 4
^{1}H NMR (300.1 MHz, $CdCl_3$): δ_H 7.71 (1H, t, $^3J_{HH}$ 7.7 Hz; ArH), 7.39 (2H, d, ^{3}JHH 7.8 Hz; 2 × ArH), 7.36 (4H, d, $^3J_{HH}$ 8.2 Hz; 4 × ArH), 7.30 (4H, d, $^3J_{HH}$ 8.2 Hz; 4 × ArH), 4.66 (4H, s; 2 × CH_2), 4.63 (4H, s; 2 × CH_2), 3.87 (4H, s; 2 × CH_2), 1.46 (4H, br s; 2 × NH_2); ^{13}C NMR (75.5 MHz, $CdCl_3$): δ_C 158.1 (ArC), 143.1 (ArC), 137.4 (ArCH), 136.5 (ArC), 128.3 (ArCH), 127.3 (ArCH), 120.1 (ArCH), 73.2 (CH_2), 72.9 (CH_2), 46.5 (CH_2); MS (ES^+) m/z 374 (50), 378 ([M+H]$^+$, 100), 400 (47); HRMS (ES^+) m/z calculated for $C_{23}H_{27}N_3O_2Na$ [M+Na]$^+$ 400.2001, found 400.2005.

N-(4-(4-(2,5-Dioxo-2,5-dihydro-1H-pyrrol-1-yl)phenethyl)phenyl)-3,5- dimethylbenzamide 5
M.p. = 229.3 – 231.4 °C; ^{1}H NMR (400.1 MHz, $CdCl_3$): δ_H 7.81 (1H, s; NH), 7.57 – 7.54 (2H, m; 2 × ArH), 7.46 (2H, s; 2 × ArH), 7.29 – 7.27 (2H, m; 2 × ArH), 7.25 – 7.22 (2H, m; 2 × ArH), 7.19 – 7.17 (3H, m; 3 × ArH), 6.84 (2H, s; 2 × CH), 2.97 – 2.89 (4H, m; 2 × CH_2), 2.38 (6H, s; 2 × CH_3); ^{13}C NMR (100.6 MHz, $CdCl_3$): δ_C 169.8 (C=O), 166.1 (C=O), 141.8 (ArC), 138.6 (ArC), 137.7 (ArC), 136.2 (ArC), 135.2 (ArC), 134.3 (CH), 133.5 (ArCH), 129.4 (ArCH), 129.2 (ArC), 129.1 (ArCH), 126.1 (ArCH), 124.9 (ArCH), 120.4 (ArCH), 37.7 (CH_2), 37.3 (CH_2), 21.4 (CH_3); MS (ES^+) m/z 447 ([M+Na]$^+$, 75), 479 (100); HRMS (ES^+) m/z calculated for $C_{27}H_{24}N_2O_3Na$ [M+Na]$^+$ 447.1685, found 447.1674.

N-(4-(4-(2,5-Dioxo-2,5-dihydro-1H-pyrrol-1-yl)phenethyl)phenyl)-3,5- bis(trifluoromethyl)benzamide 6
M.p. = 249.5 – 251.3 °C; ^{1}H NMR (300.1 MHz, d_6-DMSO): δ_H 10.6 (1H, s; NH), 8.61 (2H, s; 2 × ArH), 8.36 (1H, s; ArH), 7.68 (2H, d, $^3J_{HH}$ 8.6 Hz; 2 × ArH), 7.34 (2H, d, $^3J_{HH}$ 8.5 Hz; 2 × ArH), 7.27 (2H, d, $^3J_{HH}$ 8.6 Hz; 2 × ArH), 7.22 (2H, d, $^3J_{HH}$ 8.5 Hz; 2 × ArH), 7.17 (2H, s; 2 × CH), 2.98 –2.87 (4H, m; 2 × CH_2); ^{13}C NMR (100.6 MHz, d_6-DMSO): δ_C 170.4 (C=O), 162.7 (C=O), 141.5 (ArC), 137.8 (ArC), 137.5 (ArC), 136.7 (ArC), 135.0 (CH), 130.8 (q, $^2J_{CF}$ 33.2 Hz, ArC), 129.3 (ArC), 128.7 (ArCH), 128.2 (ArCH), 128.1 (m; ArCH), 126.4 (ArCH), 124.7 (m; ArCH), 123.5 (q, $^1J_{CF}$ 276.6 Hz; CF_3), 120.2 (ArCH), 36.9 (CH_2),36.7 (CH_2); ^{19}F NMR (376.5 MHz, d_6-DMSO) : δ_F −61.7 ($ArCF_3$); MS (ES^-) m/z 531.1 ([M−H]$^-$, 100); HRMS (ES^-) m/z calculated for $C_{27}H_{17}N_2O_3F_6$ [M-H]$^-$ 531.1143, found 531.1140.

Macrocycle cMDG
A solution of amine derivative **3** (0.5 g, 1.45 mmol) and 5-tert-butylisophthaloyl dichloride **2** (0.38 g, 1.45 mmol) in dry THF (100 mL) were added simultaneously over 1 h to a solution of Et_3N (1.25 mL, 8.71 mmol) in dry THF (82 mL) and left stirred at ambient temperature under N_2 atmosphere for 3 days. The reaction mixture was concentrated by evaporation under reduced pressure and diluted with CH_2CI_2. The solution was then washed successively with 1M HCI and 1M KOH. The organic layers were dried with $MgSO_4$ and concentrated in vacuo. The residue was purified by column chromatography (Hexane:EtOAc, 1:1) to yield macrocycle cMDG as a colorless solid (81 mg, 11%). M.p. = 247.8 – 250.4 °C; ^{1}H NMR (400.1 MHz, $CdCI_3$): δ_H 8.10 (2H, d, $^3J_{HH}$ 1.5 Hz; 2 × NH), 7.53 (1H, br s; ArH), 7.30 (8H, s; 8 × ArH), 6.43 (2H, br s; 2 × ArH), 4.57 (4H, d, $^3J_{HH}$ 5.4 Hz; 2 × CH_2), 4.50 (4H, s; 2 × CH_2), 3.58 – 3.68 (8H, m; 4 × CH_2), 1.37 (9H, s; 3 × CH_3); ^{13}C NMR (75.5 MHz, $CDCI_3$): δ_C 167.3 (C=O), 153.2 (ArC), 137.8 (ArC), 137.4 (ArC), 134.7 (ArC), 128.8 (ArCH), 128.5 (ArCH), 128.4 (ArCH), 120.6 (ArCH), 73.1 (CH_2), 70.7 (CH_2), 69.6 (CH_2), 44.3 (CH_2), 35.3 (qC), 31.3 (CH_3); MS (ES^+) m/z 553.1 ([M+Na]$^+$, 100) 554.2 (30); HRMS (ES^+) m/z calculated for $C_{32}H_{38}N_2O_5Na$ [M+Na]$^+$ 553.2678, found 553.2664.

Macrocycle cMP

A solution of amine derivative **4** (0.6 g, 1.59 mmol) and 5-tert-butylisophthaloyl dichloride **2** (0.42 g, 1.59 mmol) in dry THF (100 mL) were added simultaneously over 2 h to a solution of Et_3N (1.3 mL, 9.36 mmol) in dry THF (95 mL) and left stirred at ambient temperature under N_2 atmosphere for 3 days. The reaction mixture was concentrated in vacuo and diluted with CH_2CI_2. The solution was then washed successively with 1M HCI and 1M KOH. The organic layers were dried with $MgSO_4$ and concentrated in vacuo. The residue was purified by column chromatography (Hexane:EtOAc, 1:1) to yield macrocycle cMP as a colorless solid (100 mg, 11%). M.p. = 256.3 – 258.9 °C; ^{1}H NMR (500.1 MHz, $CdCI_3$): δ_H 8.07 (2H, d, $^3J_{HH}$ 1.4 Hz; 2 × NH), 7.71 (1H, t, $^3J_{HH}$ 7.8 Hz; ArH), 7.57 (1H, s; ArH), 7.36 (2H, d, $^3J_{HH}$ 7.8 Hz; 2 × ArH), 7.31 (8H, s; 8 × ArH), 6.39 (2H, br s; 2 × ArH), 4.65 (4H, s; 2 × CH_2), 4.58 (4H, d, $^3J_{HH}$ 5.5 Hz; 2 × CH_2), 4.42 (4H, s; 2 × CH_2), 1.37 (9H, s; 3 × CH_3); ^{13}C NMR (100.6 MHz, $CdCI_3$): δ_C 167.3 (C=O), 157.4 (ArC), 152.9 (ArC), 137.6 (ArC), 137.3 (ArCH), 137.2 (ArC), 134.6 (ArC), 129.0 (ArCH), 128.7 (ArCH), 128.1 (ArCH), 120.8 (ArCH), 120.3 (ArCH), 72.2 (CH_2), 71.5 (CH_2), 44.3 (CH_2), 35.3 (q), 31.2 (CH_3); MS (ES^+) m/z 586.1 ($[M+Na]^+$, 100); HRMS (ES^+) m/z calculated for $C_{35}H_{37}N_3O_4Na$ $[M+Na]^+$ 586.2682, found 586.2684.

Results and Discussion

The *tert*-butyl macrocycle based on diethylene glycol (MDG) was constructed from 5-*tert*-butylisophthalic acid (**1**) which was activated to acid chloride derivatives (**2**) using thionyl chloride in toluene as outlined in literature [18]. The acyl chloride (**2**) was subsequently coupled to the bis amine compound (**3**) to give the macrocycle cMDG (11%) and outlined in Scheme 1. The synthesis of the analogous framework of the control macrocycle has been reported by others [19-22].

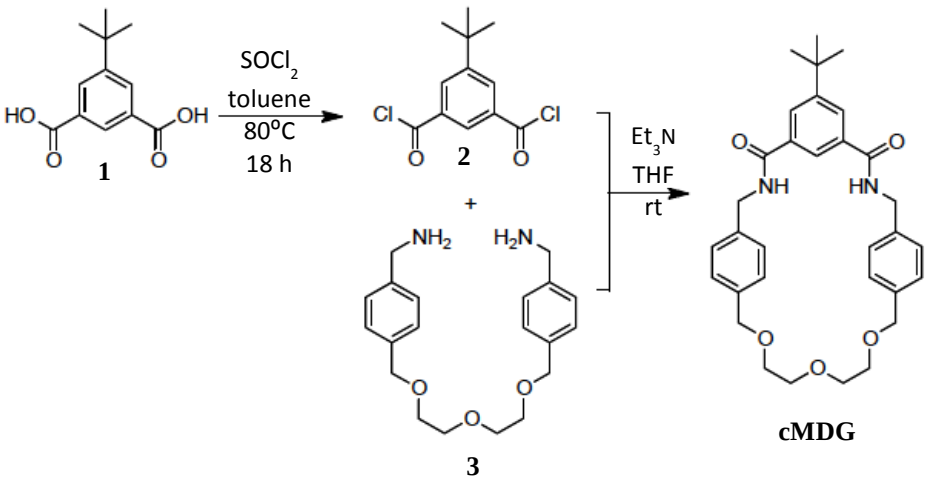

Scheme 1. Synthesis of macrocycle cMDG

Following this, we examined its calculated structure (Figure 3) to model the behavior of its structure. The opposite orientation of one of the carbonyl group in the upper fragment and the position of the diethylene glycol unit give rise to a bigger cavity in this new macrocycle.

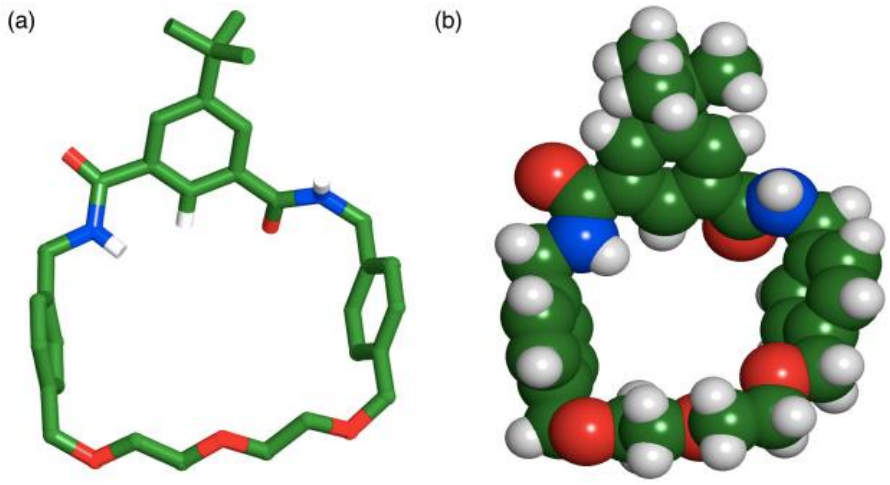

Figure 3. (a) Stick representation and (b) space filling model of the calculated structure (OPLS2005, GB/SA $CHCl_3$) of two preferable conformations for macrocycle cMDG. Carbon atoms are coloured green, oxygen atoms in red, nitrogen atoms in blue and hydrogen atoms in white (most hydrogen atoms have been removed for clarity)

Subsequently, the synthesis of the second *tert*-butyl macrocycle comprising pyridine moiety is encapsulated in Scheme 2. In similar way, treatment of the diacid (**1**) with thionyl chloride under dry conditions led to the formation of diacid dichloride (**2**), which then coupled to the diamine derivative (**4**), affording the macrocycle cMP in only 11% yield. Thus, using simple molecular mechanics calculation, we model the compound structure for macrocycle cMP (Figure 4). It is important to note that the yield of both cyclization step for macrocycle cMDG and cMP is significantly lower when the reactions were carried out in dichloromethane (4% yield). As might be expected, the possibility of the nucleophile attack in the amide bond formation step is relatively minimal in high dilution synthesis, but the use of the isophthaloyl building block further diminishes the efficiency of the ring closure step.

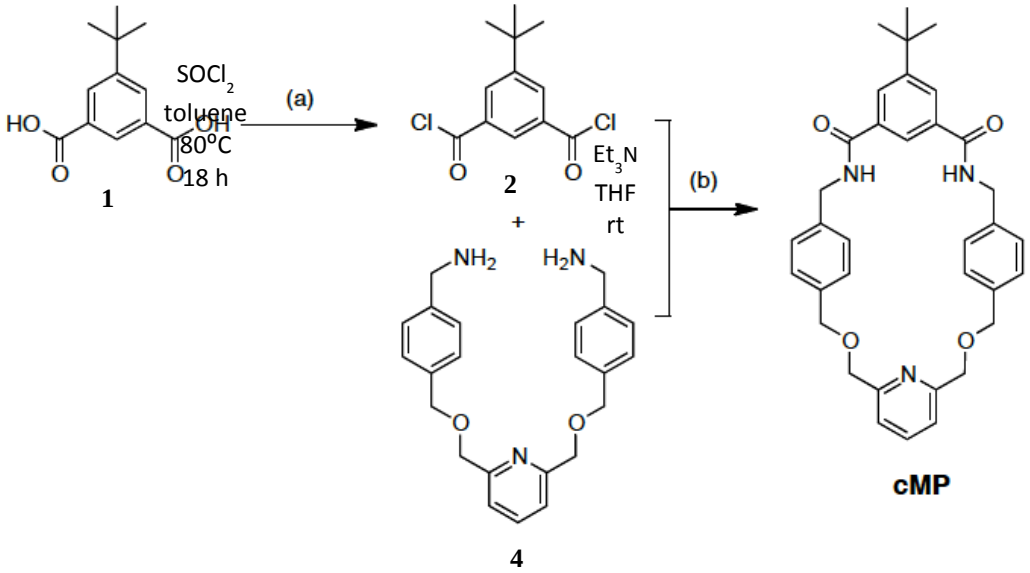

Scheme 2. Synthesis of control macrocycle cMP

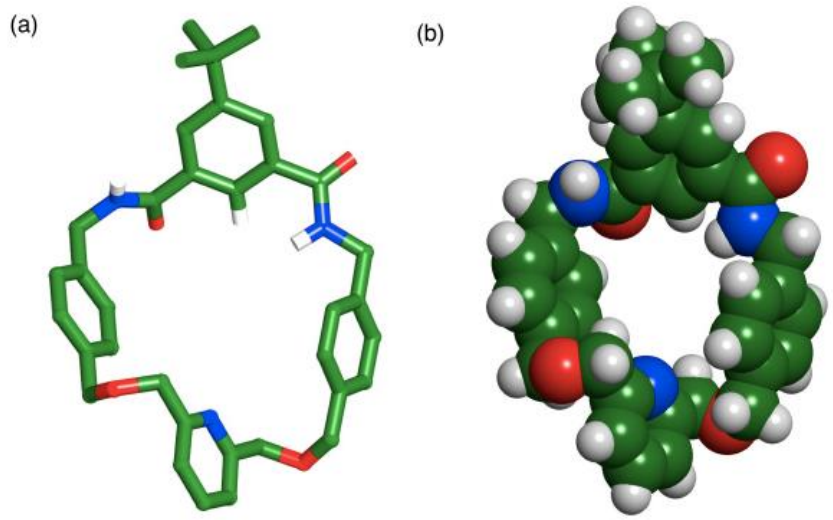

Figure 4. a) Stick representation and (b) space filling model of the calculated structure (OPLS2005, GB/SA CHCl3) of two preferable conformations for macrocycle cMDG. Carbon atoms are coloured green, oxygen atoms in red, nitrogen atoms in blue and hydrogen atoms in white (most hydrogen atoms have been removed for clarity)

Our preceding report [21] on the formation of amide macrocycle reveals the two hydrogen atoms of the amides and the electron pair of the pyridine nitrogen of the upper fragment of the macrocycle point into the interior of the macrocycle. In contrast to benzene, the electron density of the pyridine ring is not evenly distributed over the ring, reflecting the negative inductive effect of the nitrogen atom. For this reason, pyridine has a large dipole moment, which importantly influences the formation of the amide bond between the acid chloride and the amine. After the formation of the first amide bond, the other set of the acid chloride is in ideal position to aid the following nucleophilic attach and close the ring.

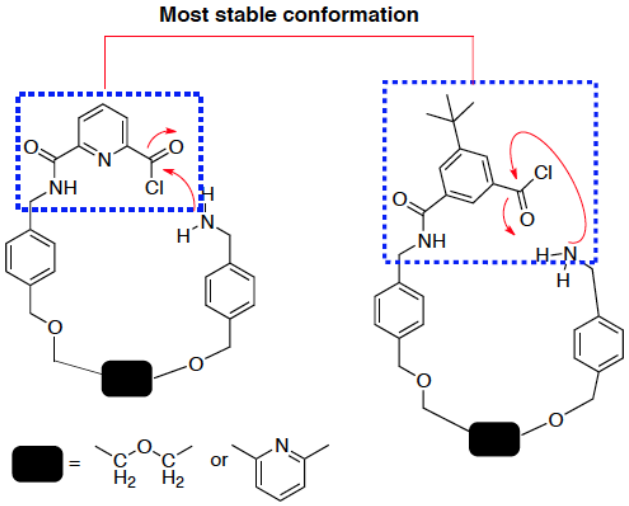

Figure 5. Possible nucleophilic acyl substitution for the ring closure for (a) macrocycle MDG or MP and (b) macrocycle cMDG or cMP

Additionally, the representation of the molecular structure for macrocycle cMDG (Figure 3) and cMP (Figure 4) reveals that their cavities are substantially larger than the parent macrocycles as a result of the absence of nitrogen atom in the upper fragment of their frameworks. The ability of these control macrocycles to complex with the potential guests is quantitatively tested in the following section.

Binding studies

Additional investigations must be conducted to evaluate the influence of the benzene ring in the framework of both control macrocycles in order to test its ability to complex the guests. In order to address this possibility, the following binding experiments were carried out with maleimide **5** and CF_3 maleimide **6**. An equimolar mixture of macrocycle cMDG and maleimide **5** in $CDCl_3$ was initially prepared and analysed by ^{1}H NMR spectroscopy. Some of the resonances of [cMDG□**5**] are rather broad at 25 °C with notable chemical shift changes, which corresponds to the pseudorotaxane formation (Figure 6a). The typical downfield shift (+1.15 ppm) of the NH macrocycle protons H8R, the upfield shift for the macrocycle phenylene protons, H11R and H12R (−0.57 ppm and −0.68 ppm) and the upfield shift for the macrocycle methylene protons H14R (−0.36 ppm) are noted. In addition, we recognized that the CH_3 resonance of maleimide **5** is separated into two sharp resonances, which corresponds to the unbound and bound state of maleimide **5**. This separation allows us to measure the association constant using the single-point method and we concluded that cMDG are capable of binding the maleimide **5** with a K_a value of 190 ± 20 M^{-1} at 25 °C in $CDCl_3$. An equimolar mixture of macrocycle cMDG and maleimide **6** in $CDCl_3$ was subsequently prepared. The 400.1 MHz ^{1}H NMR spectrum (Figure 6c) shows that the exchange resulting from the complexation and decomplexation rate of maleimide **6** is slow on the ^{1}H NMR chemical shift timescale and exhibits significant changes in chemical shifts upon the pseudorotaxane formation.

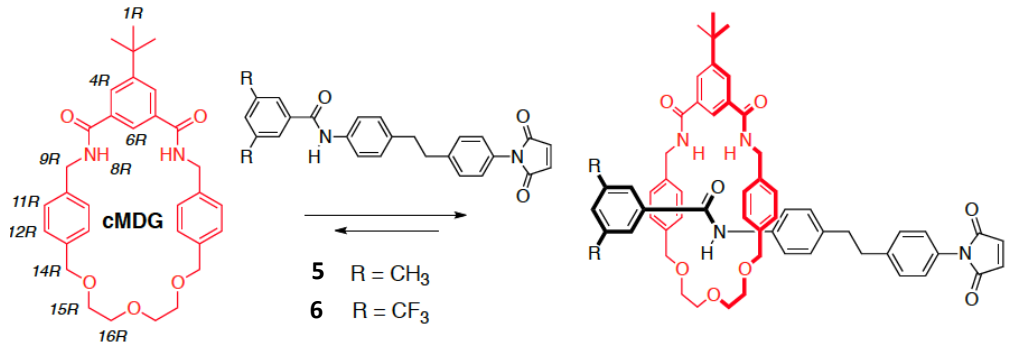

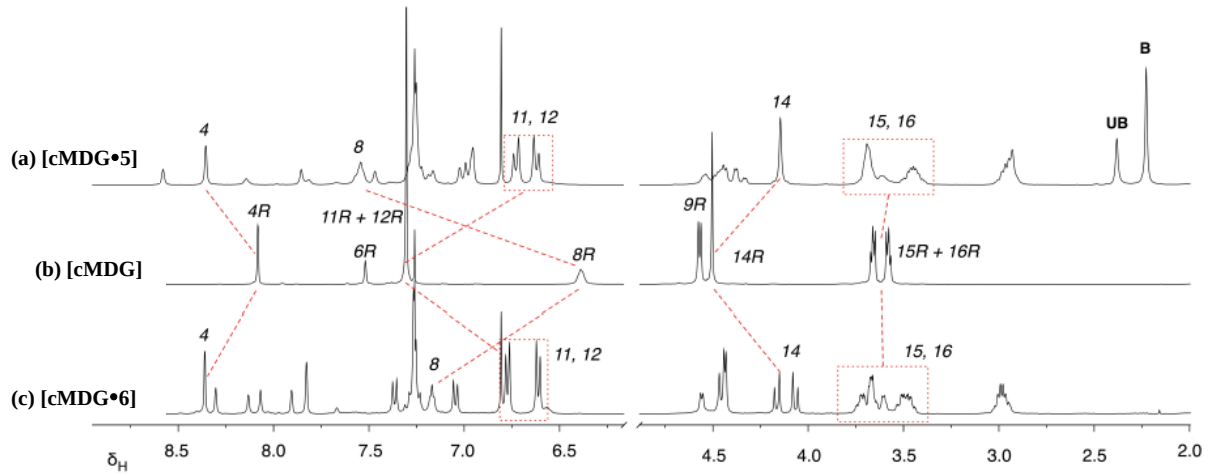

Figure 6. Partial 1H NMR spectra (300.1 MHz, 25 °C, $CDCl_3$, 20 mM) of (a) an equimolar mixture of macrocycle cMDG and maleimide **5** (b) macrocycle cMDG and (c) an equimolar mixture of macrocycle cMDG and maleimide **5**. R stands for ring component and in this case the macrocycle cMDG. Red dashed lines are shown to connect resonances for specific protons in bound and unbound states. UB stands for unbound species and B corresponds to bound species. ($\Delta\delta = \delta$unbound – δbound).

The resonance arising from the macrocycle NH protons, H8R, is again moved downfield (+0.78 ppm) as a result of the hydrogen bonding between these protons and the carbonyl group of the maleimide 110 and the characteristic upfield shifts of the macrocycle phenylene protons, H11R and H12R (−0.53 ppm and −0.69 ppm) residing in the shielding zone of an aromatic ring. Moreover, the macrocycle methylene protons H14R (singlet at δ_H 4.51 in the free macrocycle) give rise to an AB system at δ_H 4.12. From the ^{19}F NMR spectroscopy (376.5 MHz), the association constant for [cMDG•**6**] complex was estimated to be 1000 ± 100 M^{-1} at 25 °C in $CDCl_3$. The next step is to conduct the similar binding experiment in the presence of macrocycle cMP. An equimolar mixture of macrocycle cMP and maleimide **5** was prepared and analysed by ^1H NMR spectroscopy. The 300.1 MHz ^1H NMR spectrum, (Figure 7 a) shows that the [cMP•**5**] complex is near to a slow exchange process and a corresponding downfield shift of the macrocycle NH protons, H8R (+1.29 ppm) was noticed together with the upfield shifts of the macrocycle phenylene protons, H11R and H12R (−0.41 and −0.56 ppm, respectively). The association constant for the complexation of [cMDG•**5**] are determined similarly using the ^1H NMR single-point method and obtained a K_a value of 160 ± 20 M^{-1}. Binding experiment was performed next with maleimide **6**. The 400.1 MHz ^1H NMR spectrum of an equimolar mixture of macrocycle cMP and guest **6** in $CDCl_3$ (Figure 7 c) again displays a slow exchange process on the ^1H NMR chemical shift timescale. The resonances arising from NH8R is shifted downfield (+0.95 ppm), and the upfield shifts for both H11R and H12R (−0.49 and −0.56 ppm) are comparable with earlier observation in the presence of macrocycle cMDG. The macrocycle methylene protons resonances H9R, H14R and H15R are rendered magnetically inequivalent as a consequence of the unsymmetrical nature of maleimide **6**, leading to distinct complex patterns. The association constant for [cMP•**6**] complex was estimated to be 460 ± 50 M^{-1}.

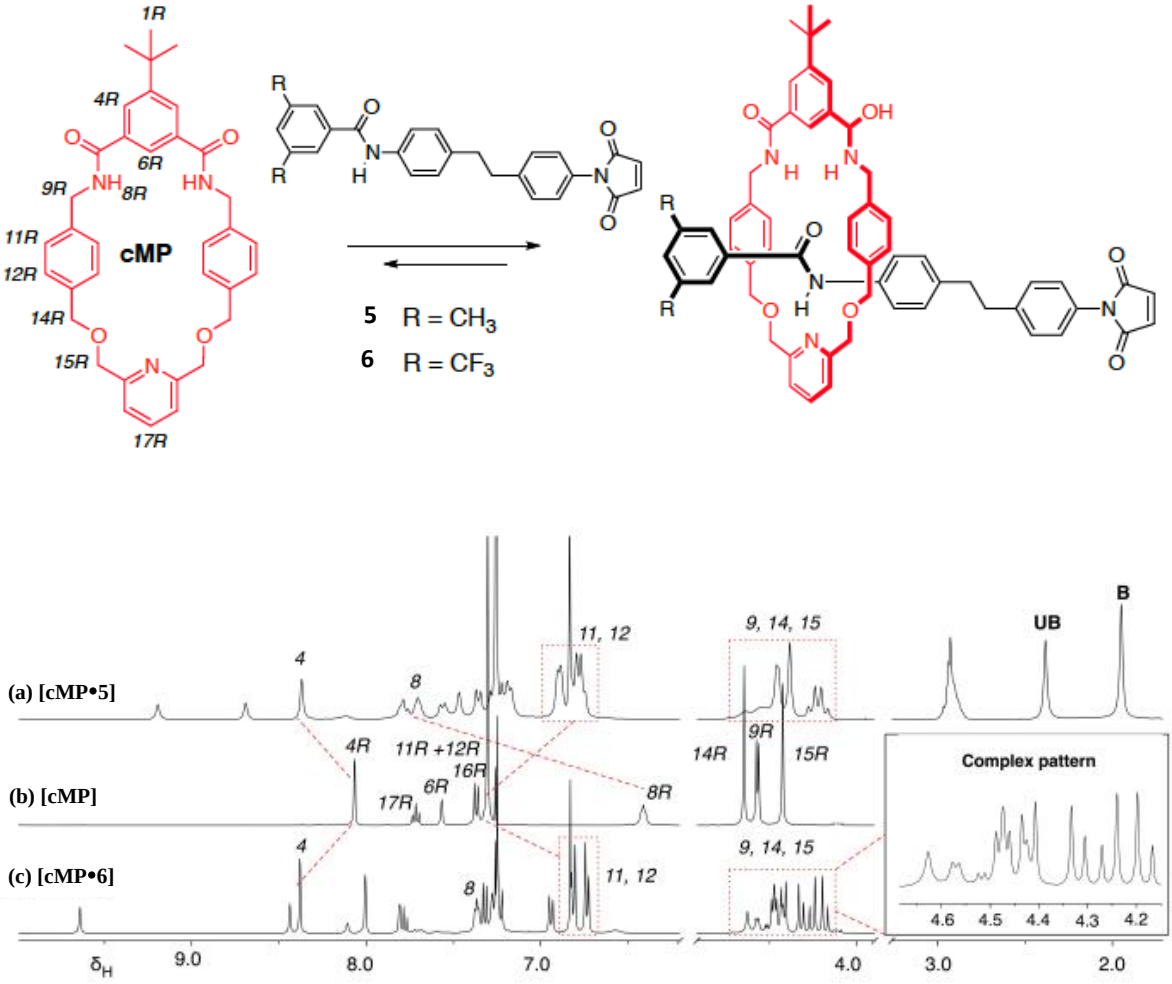

Figure 7. Partial ^{1}H NMR spectra (300.1 MHz, 25 °C, CDCl3, 20 mM) of (a) an equimolar mixture of macrocycle cMP and maleimide **5** (b) macrocycle cMP and (c) an equimolar mixture of macrocycle cMP and maleimide **6**. R stands for the ring component and in this case, the macrocycle cMP. Red dashed lines are shown to connect resonances for specific protons in bound and unbound states. UB stands for unbound species and B corresponds to bound species. (Δδ = δunbound – δbound).

We realised that the association constant, K_a for [cMDG•**6**] complex is attributed to the lower fragments of the macrocycle participating in the binding event. We reasoned that the cavity of cMP is responsible for the insufficient preorganisation of maleimide **6** as a result of the loss of rigidity of the parent macrocycle MP containing pyridine moiety. In both pseudorotaxane assembly, the influence of rapid threading and dethreading process is evident and can be discerned from the NMR spectrum. The exchange between these processes were found slow on the ^{1}H NMR chemical shift timescale, yielding a spectrum containing two populated resonances corresponds with the relative amounts of each species, bound and unbound. The complex pattern from H9R, H14R and H15R are characteristics of the emergence of the pseudorotaxane species in solution. The outcomes for the binding experiments are summarized in Table 1.

Table 1. Binding assessments conducted with control macrocycle cMDG and cMP. The ^{1}H NMR spectrum of the macrocycle and guest showed complex is in slow exchange (S) that can be attributed to significant binding events, compared to the free species observed in isolation. In the case of slow exchange, the K_a was determined using the single-point method (#) either by ^{1}H NMR or ^{19}F NMR resonance (Relaxation time, d1 is 6 sec). The concentration used was 20 mM in $CDCl_3$ at 25 °C unless otherwise stated.

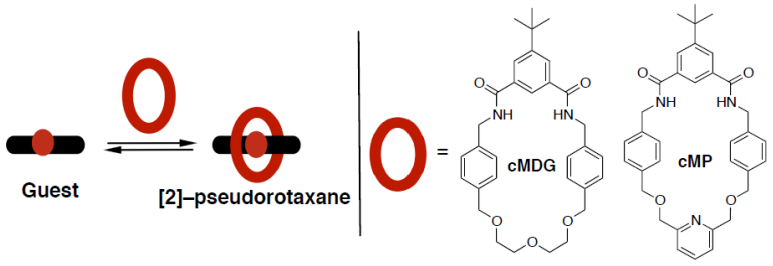

Maleimide Guest	K_a / M^{-1} (cMDG)	K_a / M^{-1} (cMP)
5	S#	S#
	K_a = 190 ± 20	K_a = 160 ± 20
6	S#	S#
	K_a = 1000 ± 100	K_a = 460 ± 50

Conclusion

The control macrocycles cMDG and cMP binds both maleimide **5** and **6** within the [2]-pseudorotaxanes assembly with a K_a value range from 160 – 1000 M^{-1}. The slow exchange process highlights the effect of the unsymmetrical nature of the maleimide component. A more complete evaluation on the effects of certain basic structural relationships on the abilities of the guest compound to thread the cavity of the macrocycle is currently being investigated.

Acknowledgement

The financial support for this work was provided by ESPRC (Grant EP/E017851/1) and GUP-2016-059. The authors acknowledge the School of Chemistry, University of St Andrews for providing facilities to carry out this research.

References

1. Hassan, N. I., del Amo, V., Calder, E. and Philp, D. (2011). Low temperature capture of pseudorotaxanes. *Organic Letters*, 13(3): 458-461.
2. Wisner, J. A., Beer, P. D. and Drew, M. G. B. (2011). A demonstration of anion templation and selectivity in pseudorotaxane formation. *Angewandte Chemie International Edition*, 40: 3606.
3. Kavallieratos, K., de Gala, S. R., Austin, D. J. and Crabtree, R. H. (1997). A readily available non-preorganized neutral acylic halide receptor with an unusual nonplanar binding conformation. *Journal of the American Chemical Society*, 119: 2325.
4. Kavallieratos, K., Bertao, C. M. and Crabtree, R. H. (1999). Hydrogen bonding in anion recognition: A family of versatile, non-preorganized neutral and acyclic receptors. *Journal of Organic Chemistry* 64: 1675.
5. Ashton, P. R., Ballardini, R., Balzani, V., Boyd, S. E., Credi, A., Gandolfi, M. T., Gomez-Lopez, M.; Iqbal, S., Philp, D., Preece, J. A., Prodi, L., Ricketts, H. G., Stoddart, J. F., Tolley, M. S., Venturi, M., White, A. J. P. and Williams, D. J. (1997). Simple mechanical molecular and supramolecular machines: photochemical and electrochemical control of switching processes. *Chemistry – a European Journal*, 3: 152.
6. Martinez-Diaz, M. V., Spencer, N. and Stoddart, J. F. (1997). The self-assembly of a switchable [2]rotaxane. *Angewandte Chemie International Edition*, 36: 1904.

7. Gaviña, P. and Sauvage, J.-P. (1997). Transition-metal template synthesis of a rotaxane incorporating two different coordinating units in its thread. *Tetrahedron Letters*, 38: 3521.
8. Mulder, A., Jukovic, A., Lucas, L. N., van Esch, J., Feringa, B. L., Huskens, J. and Reinhoudt, D. N. (2002). A dithienylethene-tethered beta-cyclodextrin dimer as a photoswitchable host. *Chemical Communications*, 75(22): 2734.
9. Illuminati, G. and Mandolini, L. (1998). Ring closure reactions of bifunctional chain molecules. *Accounts of Chemical Research* 14: 95.
10. Lindoy, L. F. (1989). The chemistry of macrocyclic ligand complexes. Cambridge University Press, England.
11. Steed, J. W. and Atwood, J. L. (2000). Supramolecular chemistry. John Wiley & Sons, Ltd, England.
12. Vidonne, A. and Philp, D. (2008). Integrating replication processes with mechanically interlocked molecular architectures, *Tetrahedron*, 64: 8464.
13. Alvarez-Pérez, M., Goldup, S. M., Leigh, D. A. and Slawin, A. M. Z. (2008). A chemically-driven molecular information ratchet. *Journal of the American Chemical Society*, 130: 1836.
14. Altieri, A., Aucagne, V., Carrillo, R., Clarkson, G. J., D'Souza, D. M., Dunnett, J. A., Leigh, D. A. and Mullen, K. M. (2011), Sulfur-containing amide-based [2]rotaxanes and molecular shuttles. *Chemical Science*, 2: 1922.
15. Vidonne, A., Kosikova, T. and Philp, D. (2016). Exploiting recognition-assembly and reactivity in [2]-rotaxane formation. *Chemical Science*, 7(4): 2592.
16. Stewart, J. J. P. (1989). Optimization of parameters for semiempirical methods II. Applications. *Journal of Computational Chemistry*, 10(2): 221.
17. Stewart, J. J. P. MOPAC (2009). Stewart Computational Chemistry, Colorado Springs, CO, USA Access from http://openmopacnet.
18. Ito, J. -I., Miyakawa, T. and Nishiyama, H. (2016). Carbon−carbon bond formation on a bis (oxazolinyl) phenyl− rhodium complex in a reduction and oxidative addition sequence. *Organometallics*, 25(22): 5216.
19. Berna, J., Brouwer, A. M., Fazio, S. M., Haraszkiewicz, N., Leigh, D. A. and Lennon, C. M. (2007). A rotaxane mimic of the photoactive yellow protein chromophore environment: effects of hydrogen bonding and mechanical interlocking on a coumarin amide derivative. *Chemical Communications*, 2007: 1910.
20. Leigh, D. A. and Thomson, A. R. (2006). Switchable dual binding mode molecular shuttle. *Organic Letters* 8(23): 5377.
21. Vickers, M. S. and Beer, P. D. (2007). Anion template assembly of mechanically interlocked structures. *Chemical Society Reviews*, 36: 211.
22. Sambrook, M. R., Beer, P. D., Wisner, J. A., Paul, R. L., Cowley, A. R., Szemes, F. and Drew, M. G. B. (2005). Anion-templated assembly of pseudorotaxanes: Importance of anion template, strength of ion-pair thread association, and macrocycle ring size. *Journal of the American Chemical Society*, 127: 2292.
23. Koulov, A. V., Mahoney, J. M. and Smith, B. D. (2003). Facilitated transport of sodium or potassium chloride across vesicle membranes using a ditopic salt-binding macrobicycle. *Organic and Biomolecular Chemistry*, 1: 27.
24. Vidonne, A. (2009). Exploiting recognition-assembly and reactivity in [2]-rotaxane formation. Thesis of PhD Degree, University of St. Andrews, Scotland.